# Transition metal atoms M (M = Fe, Co, Cu, Cr) doping and oxygen vacancy modulated M-$Ni_5P_4$-NiMOH nanosheets as multifunctional electrocatalysts for efficient overall water splitting and urea electrolysis reaction

Yanhong Wang [a], Chenyi Zhang [a], Xiaoqiang Du[a*] and Xiaoshuang Zhang[b]

a School of Chemical Engineering and Technology, North University of China, Taiyuan 030051, People's Republic of China. E-mail: duxq16@nuc.edu.cn

b School of Science, North University of China, Taiyuan 030051, People's Republic of China.

**DFT computation details:** The DFT calculations were performed using the Cambridge Sequential Total Energy Package (CASTEP) with the plane-wave pseudo-potential method. The geometrical structures of the (003) plane of Co-NiOOH, Cr-NiOOH, Cu-NiOOH and Fe-NiOOH was optimized by the generalized gradient approximation (GGA) methods. The Revised Perdew-Burke-Ernzerh of (RPBE) functional was used to treat the electron exchange correlation interactions. A Monkhorst Pack grid k-points of 7*7*1 of Co-NiOOH, Cr-NiOOH, Cu-NiOOH and Fe-NiOOH, a plane-wave basis set cut-off energy of 500 eV were used for integration of the Brillouin zone. The structures were optimized for energy and force convergence set at 0.05 eV/A and $2.0\times10^{-5}$ eV, respectively.

## Experiment section

### Chemicals and materials

All reagents were analytical grade and were used directly without any purification. $Ni(NO_3)_2\cdot6H_2O$, $NaH_2PO_2\cdot H_2O$, $Fe(NO_3)_3\cdot9H_2O$, $Co(NO_3)_3\cdot6H_2O$, $Cu(NO_3)_2\cdot6H_2O$, $Cr(NO_3)_3\cdot9H_2O$, urea ($CH_4N_2O$), and ammonium fluoride ($NH_4F$) were purchased from Sigma-Aldrich. Commercial nickel foam (NF) was purchased from an energy company. Deionized water was used in all experiments.

### Synthesis of precursor Co-doped $Ni(OH)_2$/NF

The Co-doped $Ni(OH)_2$/NF nanosheets were prepared by hydrothermal method. Firstly, the commercial NF (2.8 cm × 3 cm × 1 mm) was successively washed in acetone and dilute HCl

solution ($V_{H_2O}$ : $V_{HCl}$ = 1 : 2) under ultrasonication for 30 and 20 min, respectively, and followed by with water. Secondly, 0.75 mmol $Ni(NO_3)_2 \cdot 6H_2O$, 0.25 mmol $Co(NO_3)_3 \cdot 6H_2O$, 3 mmol $CH_4N_2O$, and 3 mmol $NH_4F$ were dissolved in 30 mL deionized water. Thirdly, the NF and the mixed solutions were transferred to a 45 m L-stainless-steel Teflon-lined autoclave heated at 140 ◦C for 4 h. After natural cooling to room temperature, the resultant NiCo-LDH/NF were washed thoroughly with deionized water and dried in vacuum at 60 °C for 12 h. Finally, the obtained NiCo-LDH/NF was calcinated in air at 300 °C for 30 min to form Co-doped $Ni(OH)_2$/NF (denoted as NiCoOH/NF).

**Synthesis of Co-$Ni_5P_4$/ Co-$Ni(OH)_2$/NF**

The obtained NiCoOH/NF was loaded in a quartz boat, and the $NaH_2PO_2 \cdot H_2O$ (1 g) was placed in another quartz boat. The two quartz boats were packaged by the silver papers with three small holes. Afterwards, the boats were put into a tube furnace. The furnace was purged with nitrogen ($N_2$) at a flow rate of 20 sccm for 1 h and then was heated at 350 ◦C for 2 h. The $N_2$ gas flow was maintained throughout the whole process. Finally, the NiMOH/NF were transformed to Co-$Ni_5P_4$/ Co-$Ni(OH)_2$/NF (Co-$Ni_5P_4$-NiCoOH/NF).

**Synthesis of M-$Ni_5P_4$-NiMOH (M = Fe, Cu, Cr)**

The preparation process was same as that of Co-$Ni_5P_4$-NiCoOH/NF. During the experiment, $Co(NO_3)_3 \cdot 6H_2O$ was replaced with $Fe(NO_3)_3 \cdot 9H_2O$, $Cu(NO_3)_2 \cdot 6H_2O$ , $Cr(NO_3)_3 \cdot 9H_2O$.

**Materials Characterization**

The XRD patterns were reported from a Philips 1130 X-ray diffractometer (40 kV, 30 mA, Cu KR radiation, λ=1.5418 Å). The morphology of the Co-$Ni_5P_4$-NiCoOH/NF, Fe-$Ni_5P_4$-NiFeOH/NF, Cu-$Ni_5P_4$-NiCuOH/NF and Cr-$Ni_5P_4$-NiCrOH/NF material is characterized by SEM images (Hitachi S-4800). TEM and HRTEM images were performed on a JEM-2100 with an accelerating voltage of 200 kV. The chemical composition and elemental states were analyzed by X-ray photoelectron spectroscopy (XPS, Axis Ultra DLD) using 60 W monochromated Mg Kα radiations as the exciting source.

**Electrochemical measurements**

Electrocatalytic tests were done with a CHI 760E electrochemical workstation (CH Instruments, Inc., Shanghai) in a typical three-electrode device. The resulting self-supported Co-$Ni_5P_4$-NiCoOH/NF, Fe-$Ni_5P_4$-NiFeOH/NF, Cu-$Ni_5P_4$-NiCuOH/NF and Cr-$Ni_5P_4$-NiCrOH/NF electrodes were directly utilized as working electrode, a graphite rod and Ag/AgCl as counter electrode and reference electrode, respectively. All measured potentials in this work were calibrated to RHE according to the following equation: E (RHE) = E (Ag/AgCl) + (0.197 + 0.059* pH). Linear sweep voltammetry polarization curves were performed in 1 M KOH solution at a scan rate of 5 mV $s^{-1}$. Electrochemical impedance spectra (EIS) were collected at a frequency between 100 kHz and 0.01 Hz. In water splitting tests, all results were revised by ohmic potentials drop (iR) correction. The electrolyte for OER measurements was 1 M KOH, whereas the UOR performances were evaluated in 1 M KOH with 0.5 M urea. The stability measurements were recorded by chronopotentiometry measurements.

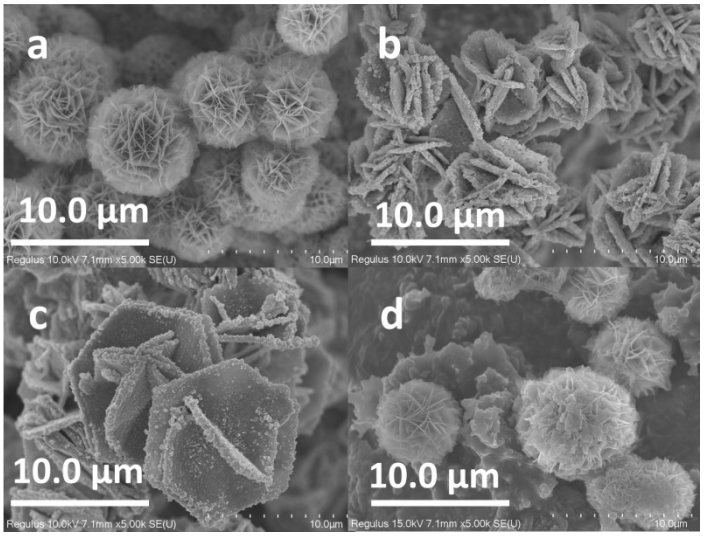


**Fig. S1.**SEM images of (a) Fe-$Ni_5P_4$-NiFeOH, (b) Co-$Ni_5P_4$-NiCoOH, (c) Cu-$Ni_5P_4$-NiCuOH and (d) Cr-$Ni_5P_4$-NiCrOH.

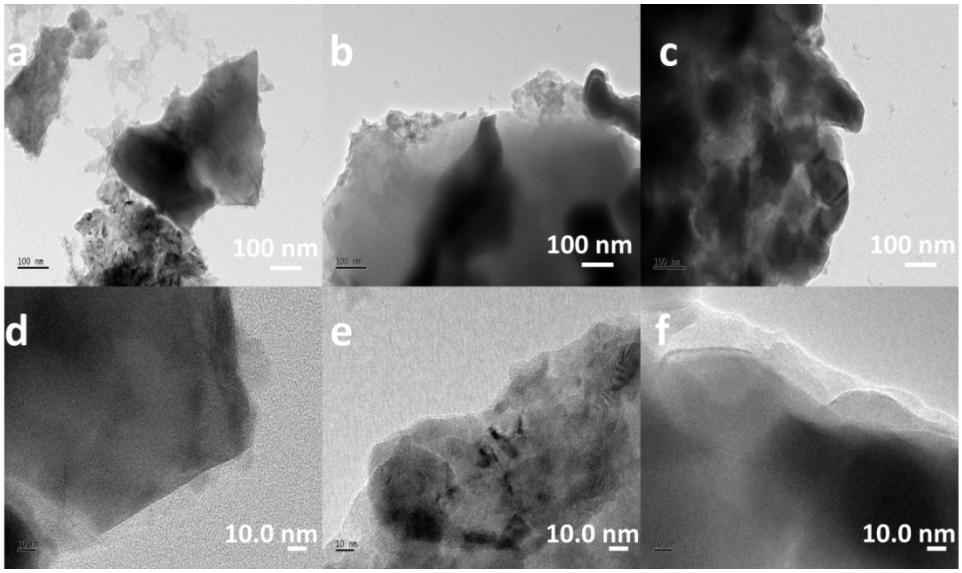


**Fig. S2.**TEM images of Co-$Ni_5P_4$-NiCoOH (a-c) 100 nm, and (d-f) 10 nm.

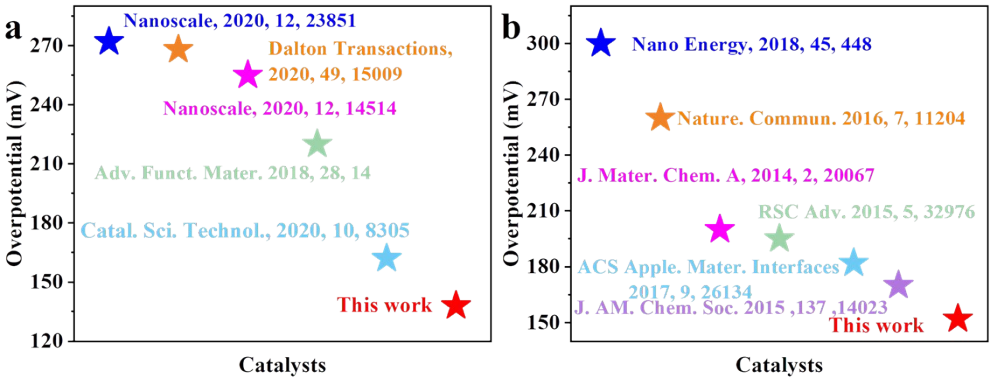


**Fig. S3**.Comparison of overpotentials of (a) OER [1-5] and (b) HER [6-11] for Co-$Ni_5P_4$-NiCoOH electrodes with reported electrocatalysts in the alkaline media.

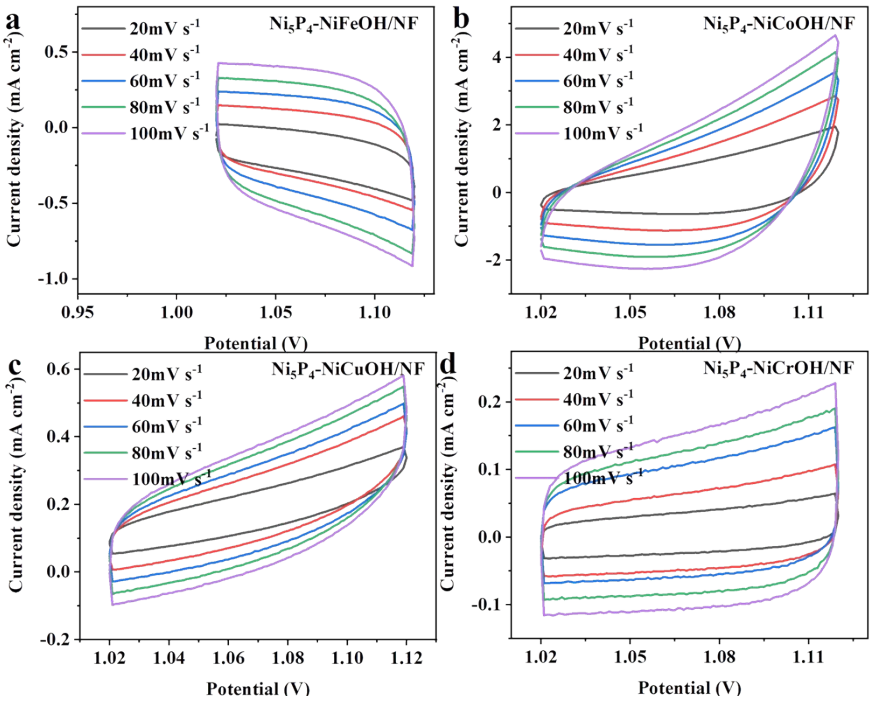


**Fig. S4**. In 1.0 M KOH, cyclic voltammograms of a) Fe-$Ni_5P_4$-NiFeOH, b) Co-$Ni_5P_4$-NiCoOH, c) Cu-$Ni_5P_4$-NiCuOH and d) Cr-$Ni_5P_4$-NiCrOH at the different scan rates varying from 20 to 100 $mV \cdot s^{-1}$for OER.

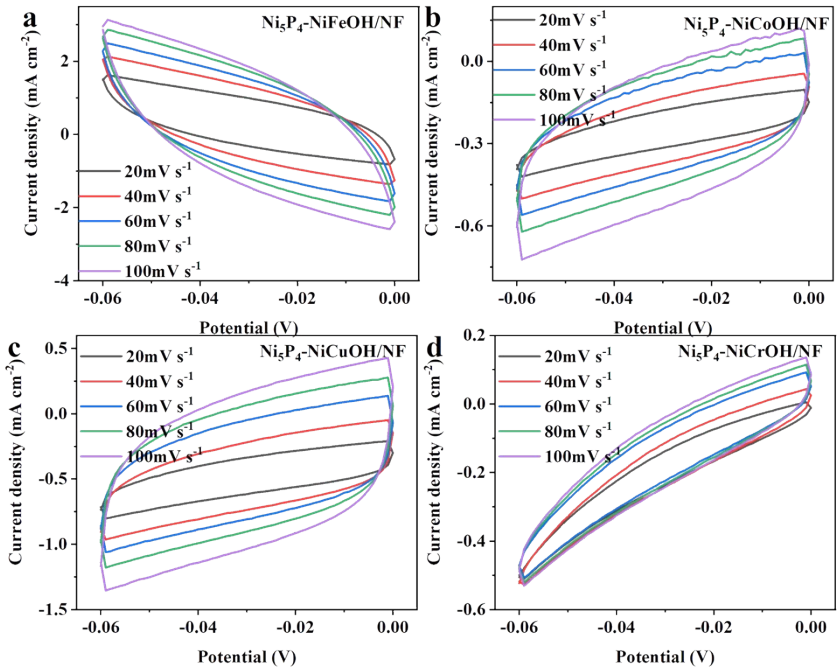


**Fig. S5**. In 1.0 M KOH, cyclic voltammograms of a) Fe-$Ni_5P_4$-NiFeOH, b) Co-$Ni_5P_4$-NiCoOH, c) Cu-$Ni_5P_4$-NiCuOH and d) Cr-$Ni_5P_4$-NiCrOH at the different scan rates varying from 20 to 100 $mV \cdot s^{-1}$ for HER.

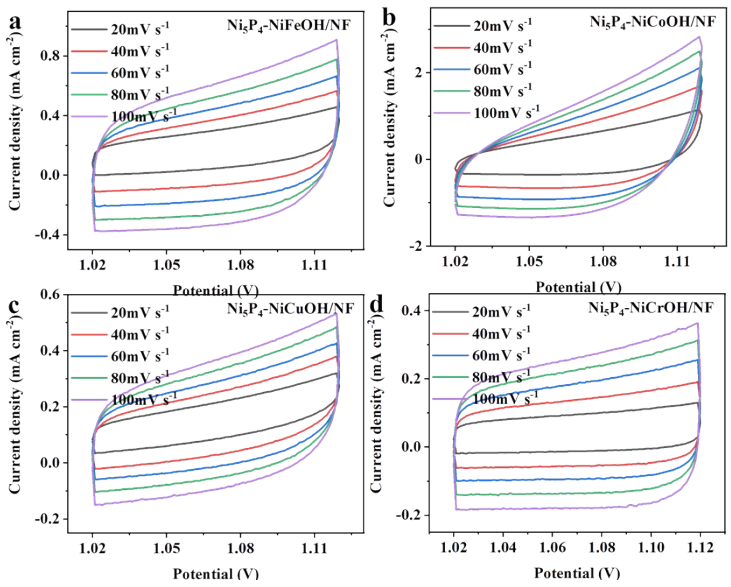


**Fig. S6**. In 1.0 M KOH with 0.5 M urea, cyclic voltammograms of a) Fe-$Ni_5P_4$-NiFeOH, b) Co-$Ni_5P_4$-NiCoOH, c) Cu-$Ni_5P_4$-NiCuOH and d) Cr-$Ni_5P_4$-NiCrOH at the different scan rates varying from 20 to 100 mV·$s^{-1}$ for UOR.

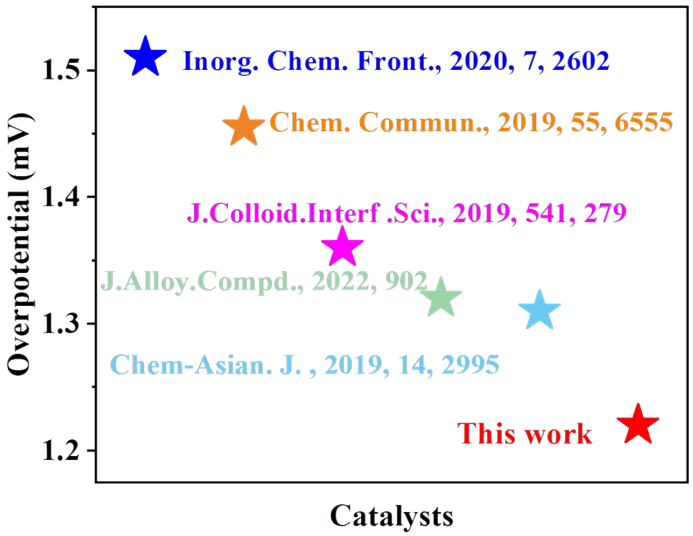


**Fig. S7**.Comparison of overpotentials of UOR [12-16] in 1M KOH + 0.5 M Urea.

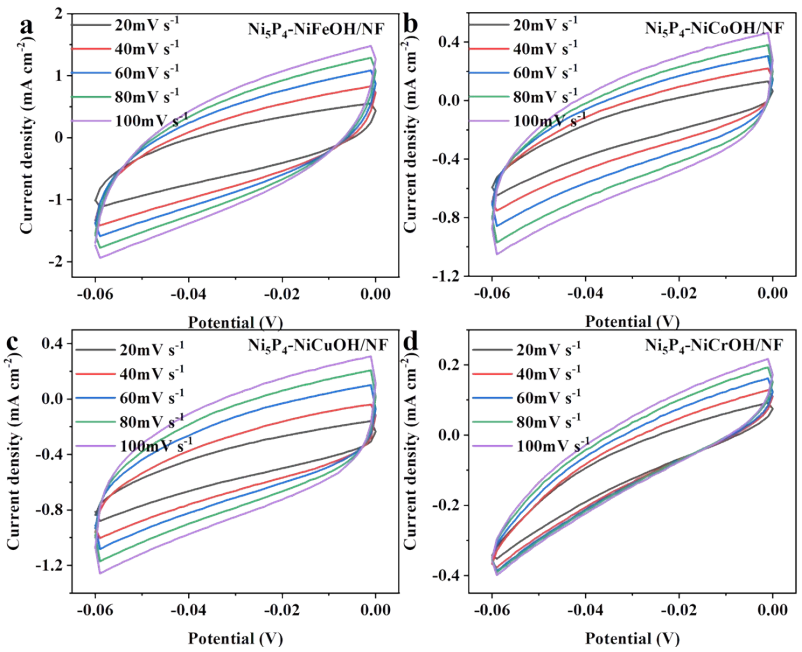


**Fig. S8**. In 1.0 M KOH with 0.5 M urea, cyclic voltammograms of a) Fe-$Ni_5P_4$-NiFeOH, b) Co-$Ni_5P_4$-NiCoOH, c) Cu-$Ni_5P_4$-NiCuOH and d) Cr-$Ni_5P_4$-NiCrOH at the different scan rates varying from 20 to 100 $mV \cdot s^{-1}$ for HER.

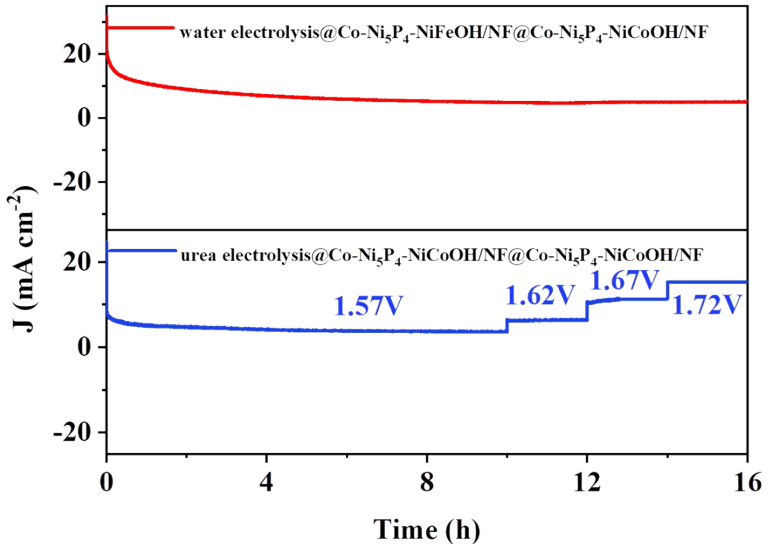


**Fig. S9**. Chronopotentiometric curve of Co-$Ni_5P_4$-NiCoOH for water electrolysis (1M KOH) and urea electrolysis (1M KOH + 0.5M Urea).

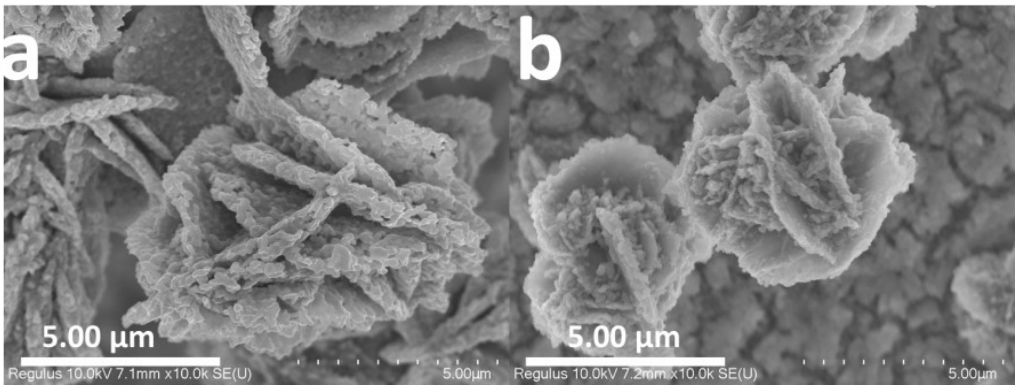


**Fig. S10**. SEM images of a) Co-$Ni_5P_4$-NiCoOH and b) Co-$Ni_5P_4$-NiCoOH after OER for 16 h.

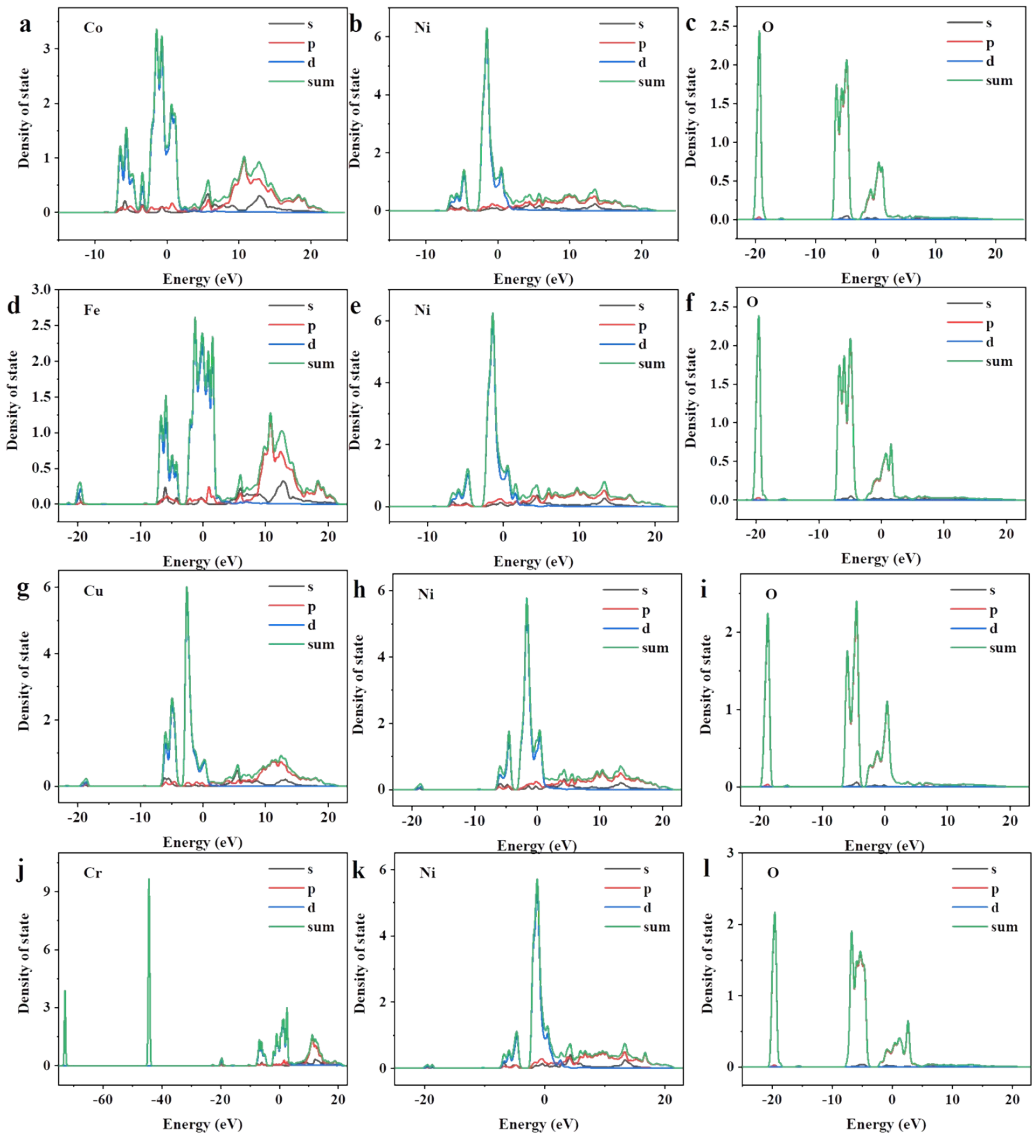


**Fig.S11.** Density of states for the Co-NiOOH, (a) Co, (b) Ni and (c) O; the Fe-NiOOH ,(d) Fe, (e) Ni and (f) O; the Cu-NiOOH, (g) Cu, (h) Ni and (i) O and the Cr-NiOOH ,(f) Cr, (g)Ni and (h) O.

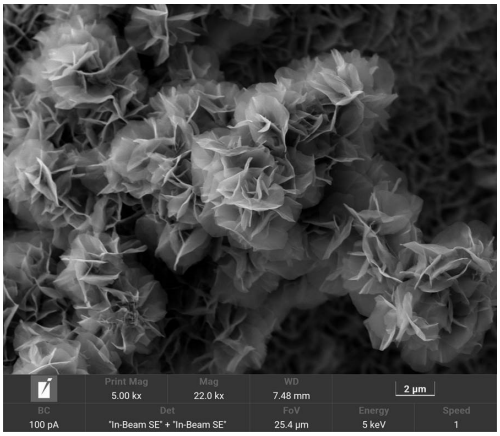


**Fig. S12.**SEM images of Co doped $Ni(OH)_2$/NF.

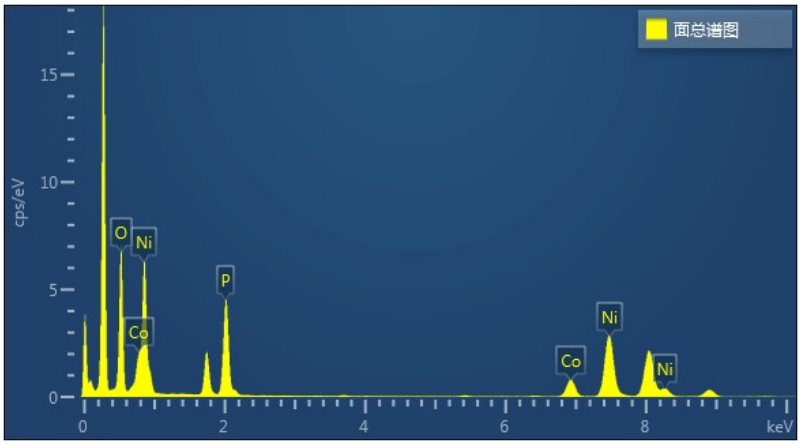


**Table S1.** Elemental composition of Co, Ni and P in the Co-$Ni_5P_4$-NiCoOH nanoarrays and by ICP. Regardless of oxygen by this characterization.

| Element | Mass fraction % | Atomic fraction % |
|---|---|---|
| Co | 10.18 | 5.36 |
| Ni | 31.68 | 15.19 |
| P | 40.17 | 10.23 |

[1] H.J. Zhang, X.P. Li, A. Hahnel, V. Naumann, C. Lin, S. Azimi, S.L. Schweizer, A.W. Maijenburg, R.B. Wehrspohn, Bifunctional Heterostructure Assembly of NiFe LDH Nanosheets on NiCoP Nanowires for Highly Efficient and Stable Overall Water Splitting;Adv. Funct. Mater., 2018;28.

[2] J.M. Huo, Y. Wang, L.T. Yan, Y.Y. Xue, S.N. Li, M.C. Hu, Y.C. Jiang, Q.G. Zhai, In situsemi-transformation from heterometallic MOFs to Fe-Ni LDH/MOF hierarchical architectures for boosted oxygen evolution reaction;Nanoscale, 2020;12: 14514-23.

[3] F.F. Yuan, Z.H. Liu, G.X. Qin, Y.H. Ni, Fe-Doped Co-Mo-S microtube: a highly efficient bifunctional electrocatalyst for overall water splitting in alkaline solution;Dalton Transactions, 2020;49: 15009-22.

[4] R. Zhang, R.L. Zhu, Y. Li, Z. Hui, Y.Y. Song, Y.L. Cheng, J.J. Lu, CoP and Ni2P implanted in a hollow porous N-doped carbon polyhedron for pH universal hydrogen evolution reaction and alkaline overall water splitting;Nanoscale, 2020;12: 23851-8.

[5] H. Zhao, M. Jiang, Q. Kang, L.Q. Liu, N. Zhang, P.C. Wang, F.M. Zhou, Electrocatalytic oxygen and hydrogen evolution reactions at Ni3B/Fe2O3 nanotube arrays under visible light radiation;Catal. Sci. Technol., 2020;10: 8305-13.

[6] J. Wang, D.F. Gao, G.X. Wang, S. Miao, H.H. Wu, J.Y. Li, X.H. Bao, Cobalt nanoparticles encapsulated in nitrogen-doped carbon as a bifunctional catalyst for water electrolysis;J. Mater. Chem. A, 2014;2: 20067-74.

[7] L.L. Feng, G.T. Yu, Y.Y. Wu, G.D. Li, H. Li, Y.H. Sun, T. Asefa, W. Chen, X.X. Zou, High-Index Faceted Ni3S2 Nanosheet Arrays as Highly Active and Ultrastable Electrocatalysts for Water Splitting;J. Am. Chem. Soc., 2015;137: 14023-6.

[8] X.L. Wu, B. Yang, Z.J. Li, L.C. Lei, X.W. Zhang, Synthesis of supported vertical NiS2 nanosheets for hydrogen evolution reaction in acidic and alkaline solution;Rsc Advances, 2015;5: 32976-82.

[9] J.S. Li, Y. Wang, C.H. Liu, S.L. Li, Y.G. Wang, L.Z. Dong, Z.H. Dai, Y.F. Li, Y.Q. Lan, Coupled molybdenum carbide and reduced graphene oxide electrocatalysts for efficient hydrogen evolution;Nat. Commun., 2016;7.

[10] C.J. Xuan, J. Wang, W.W. Xia, Z.K. Peng, Z.X. Wu, W. Lei, K.D. Xia, H.L.L. Xin, D.L. Wang, Porous Structured Ni-Fe-P Nanocubes Derived from a Prussian Blue Analogue as an Electrocatalyst for Efficient Overall Water Splitting;ACS Appl. Mate. Interfaces . 2017;9: 26134-42.

[11] Y. Zhang, Q. Shao, S. Long, X.Q. Huang, Cobalt-molybdenum nanosheet arrays as highly efficient and stable earth-abundant electrocatalysts for overall water splitting;Nano Energy, 2018;45: 448-55.

[12] F.C. Wu, G. Ou, J. Yang, H.N. Li, Y.X. Gao, F.M. Chen, Y. Wang, Y.M. Shi, Bifunctional nickel oxide-based nanosheets for highly efficient overall urea splitting;Chem. Commun., 2019;55: 6555-8.

[13] L. Yan, Y.L. Sun, E.L. Hu, J.Q. Ning, Y.J. Zhong, Z.Y. Zhang, Y. Hu, Facile in-situ growth of Ni2P/Fe2P nanohybrids on Ni foam for highly efficient urea electrolysis;J.Colloid.Interf .Sci., 2019;541: 279-86.

[14] C.Y. Zhang, T.T. Chen, H. Zhang, Z.H. Li, J.C. Hao, Hydrated-Metal-Halide-Based Deep-Eutectic-Solvent-Mediated NiFe Layered Double Hydroxide: An Excellent Electrocatalyst for Urea Electrolysis and Water Splitting;Chemistry-an Asian Journal, 2019;14: 2995-3002.

[15] H.Z. Xu, K. Ye, K. Zhu, J.L. Yin, J. Yan, G.L. Wang, D.X. Cao, Template-directed assembly of urchin-like CoSx/Co-MOF as an efficient bifunctional electrocatalyst for overall water and urea electrolysis;Inorganic Chemistry Frontiers, 2020;7: 2602-10.

[16] Q. Li, W.X. Zhang, J. Shen, X.Y. Zhang, Z. Liu, J.Q. Liu, Trimetallic nanoplate arrays of Ni-Fe-Mo sulfide on FeNi3 foam: A highly efficient and bifunctional electrocatalyst for overall water splitting;J.Alloy.Compd., 2022;902.